

## RETRIEVAL OF EFFECTIVE ELECTROMAGNETIC PARAMETERS OF ISOTROPIC METAMATERIALS USING REFERENCE-PLANE INVARIANT EXPRESSIONS

U. C. Hasar<sup>1, 2 \*</sup>, J. J. Barroso<sup>3</sup>, C. Sabah<sup>4</sup>, I. Y. Ozbek<sup>1, 2</sup>, Y. Kaya<sup>1</sup>, D. Dal<sup>5</sup>, and T. Aydin<sup>5</sup>

<sup>1</sup>Department of Electrical and Electronics Engineering, Ataturk University, Erzurum 25240, Turkey

<sup>2</sup>Center for Research and Application of Nanoscience and Nanoengineering, Ataturk University, Erzurum 25240, Turkey

<sup>3</sup>Associated Plasma Laboratory, National Institute for Space Research, São José dos Campos, SP 12227-010, Brazil

<sup>4</sup>Physikalisches Institut, J. W. Goethe Universität, Frankfurt, Germany

<sup>5</sup>Department of Computer Engineering, Ataturk University, Erzurum 25240, Turkey

**Abstract**—Three different techniques are applied for accurate constitutive parameters determination of isotropic split-ring resonator (SRR) and SRR with a cut wire (Composite) metamaterial (MM) slabs. The first two techniques use explicit analytical calibration-dependent and calibration-invariant expressions while the third technique is based on Lorentz and Drude dispersion models. We have tested these techniques from simulated scattering ( $S$ -) parameters of two classic SRR and Composite MM slabs with various level of losses and different calibration plane factors. From the comparison, we conclude that whereas the extracted complex permittivity of both slabs by the analytical techniques produces unphysical results at resonance regions, that by the dispersion model eliminates this shortcoming and retrieves physically accurate constitutive parameters over the whole analyzed frequency region. We argue that incorrect retrieval of complex permittivity by analytical methods comes from spatial dispersion effects due to the discreteness of conducting elements within MM slabs which largely vary simulated  $S$ -parameters in the resonance regions where the slabs are highly spatially dispersive.

---

*Received 24 July 2012, Accepted 11 September 2012, Scheduled 5 October 2012*

\* Corresponding author: Ugur Cem Hasar (ugur.hasar@yahoo.com).

## 1. INTRODUCTION

Metamaterials (MMs) are artificially structured composite materials with periodic cellular architecture that either mimic known material responses or produce physically realizable response functions not available in nature. The periodic sequence of identical cells having unique features results in exotic electromagnetic properties not observed by conventional materials such as negative refraction, invisible cloaks, filters, etc. [1–7]. In fabrication of these engineered materials, the lattice is arranged in such a combination that its size is much smaller than the operating wavelength [8]. By this arrangement, many unit cells reside within one-wavelength range, and thus it becomes possible to replace the overall MM structure by a homogenous and continuous medium with a well-defined wave impedance ( $z_w$ ) and refractive index ( $n$ ) [8].

To examine electromagnetic properties ( $z_w$ ,  $n$ , etc.) of MMs, various methods have been proposed for retrieval of these properties when they are exposed to an electromagnetic stimulus. Among these methods, scattering ( $S$ -) parameter material extraction methods seem promising since they allow analyses of both numerical/simulation and experiment. The Nicolson-Ross-Weir (NRW) technique as the most popular and well-known  $S$ -parameter extraction method and its variants have been applied to extract effective electromagnetic properties of not only conventional materials but also MMs (contemporary materials) [9–18]. However, it has been observed that at some frequency bands as well as for some MM configurations, retrieved effective electromagnetic properties of isotropic and bi-anisotropic MM slabs by the NRW technique exhibit some non-physical results [16, 18–20], since it relies upon retrieval of these properties of materials directly from obtained  $S$ -parameters. This problem arises due to discreteness of conducting elements repeating periodically in a MM structure in simulation programs. It can be resolved by enforcing suitable dispersion models which underlie the physical nature of MM slabs in the extraction process [19]. Furthermore, the proposed method in [19], in addition to eliminating non-physical inaccuracies, also determines effective MM parameters including electronic and magnetic resonant (plasma) frequencies, electronic and magnetic damping factors, and etc. However, it is not feasible when slab surfaces and calibration-planes do not coincide with each other. On the other hand, as a variant of the NRW technique, two reference-plane invariant methods have been recently devised to extract electromagnetic properties of conventional isotropic materials from measured  $S$ -parameters [14, 15]. In this research paper, we combine advantages of the methods

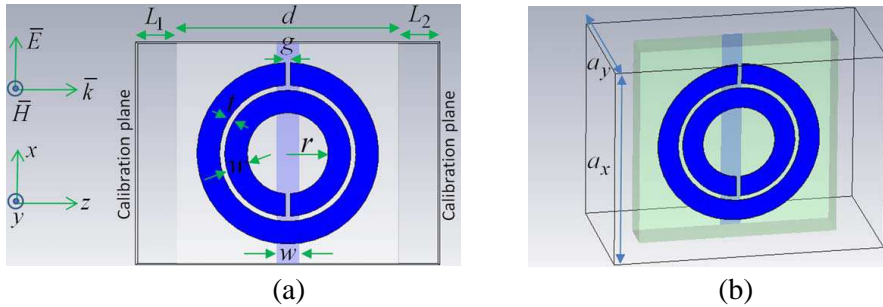


**Figure 1.** (a) A plane wave incident to a single cell of an isotropic MM slab composed of concentric circular SRRs with/without cut wires and (b) periodicity in  $x$  and  $y$  directions.

in [14, 15, 19] and propose another method for accurate retrieval of effective electromagnetic properties as well as effective parameters of isotropic MM slabs using reference-plane invariant expressions.

## 2. STATEMENT OF THE PROBLEM

The problem of determining effective electromagnetic properties of an isotropic MM slab composed of concentric circular split-ring resonators (SRRs) with/without cut wires is depicted in Fig. 1. The slabs have identical lengths of  $d = 8.8\text{mm}$  in the direction of wave travel ( $z$  direction) with theoretically infinite periodicity in  $x$  and  $y$  directions (see Fig. 1(b),  $a_x = 8.8\text{mm}$ ,  $a_y = 6.5\text{mm}$ ). It is seen from Fig. 1(a) that left and right end surfaces of the slab do not touch with calibration-planes, being apart from slab surfaces by  $L_1$  and  $L_2$ . In the analysis, it is assumed that a uniform plane wave linearly polarized in the  $x$  direction propagates along the  $z$  direction and is incident upon the slab in Fig. 1(a).

Because the direction of electric field is along the direction of slits, the MM slab in Fig. 1 does not indicate strong bi-anisotropy [18, 21]. In addition, SRRs are planar structures arranged in an infinite lattice to create a left-handed medium, producing an isotropic magnetic medium [22]. Assuming that the time dependence is of the form  $\exp(-i\omega t)$  and applying boundary conditions along  $z$  direction (continuity of tangential components of electric and magnetic fields), forward and backward reflection and transmission  $S$ -parameters at calibration-planes of the cell in Fig. 1 can be written [9–17, 19, 20]

$$S_{11} = R_1^2 \frac{\Gamma(1-T^2)}{1-\Gamma^2 T^2}, \quad S_{22} = R_2^2 \frac{\Gamma(1-T^2)}{1-\Gamma^2 T^2}, \quad S_{21} = S_{12} = R_1 R_2 \frac{T(1-\Gamma^2)}{1-\Gamma^2 T^2}, \quad (1)$$

$$\Gamma = (z_w - 1)/(z_w + 1), \quad T = e^{ik_0 nd}, \quad R_1 = e^{ik_0 L_1}, \quad R_2 = e^{ik_0 L_2},$$

$$k_0 = 2\pi f/c. \quad (2)$$

Here,  $\Gamma$  and  $T$  are, respectively, the reflection coefficient at the air-MM slab interface and the propagation factor through the MM slab;  $z_w$  and  $n$  the normalized wave impedance and the refractive index of the MM slab;  $k_0$ ,  $f$ ,  $c$  the free-space wavenumber, the operating frequency, and the velocity of light in vacuum; and  $d$ ,  $L_1$ , and  $L_2$  the length of the MM slab, and the distances between the left and right surfaces of the MM slab and the calibration-planes, respectively. We note from Eq. (1) that for an isotropic sample,  $S_{11}$  becomes not equal to  $S_{22}$  due to asymmetric calibration plane distances ( $L_1$  and  $L_2$ ). Besides, it is seen from Eqs. (1) and (2) that  $a_x$  and  $a_y$  do not enter into theoretical analysis because the slab has infinite lengths in those directions.

### 3. RETRIEVAL METHODS

Here, we will introduce three retrieval methods for extracting electromagnetic properties of isotropic MM slabs in Fig. 1 using reference-plane dependent and reference-plane invariant expressions. In the first two methods, we will utilize NRW type analytical expressions [9–17], and in the third method, we will use dispersion models [19].

#### 3.1. The Analytical Approach — Reference-plane Dependent

The analytical approach with reference-plane dependent expressions for retrieval of electromagnetic properties of isotropic MMs is based on using in Eqs. (1) and (2). From these equations, we find retrieved complex permittivity ( $\varepsilon_r$ ) and complex permeability ( $\mu_r$ ) [9, 10, 17]

$$z_w = \mp \sqrt{\frac{(1 + S_{11}/R_1^2)^2 - S_{21}^2/(R_1^2 R_2^2)}{(1 - S_{11}/R_1^2)^2 - S_{21}^2/(R_1^2 R_2^2)}}, \quad T = \frac{S_{21}/(R_1 R_2)}{1 - \frac{S_{11}}{R_1^2} \left( \frac{z_w - 1}{z_w + 1} \right)}, \quad (3)$$

$$n = n' + in'' = \frac{\text{Im}\{\ln(T)\} \pm 2\pi m - i \text{Re}\{\ln(T)\}}{k_0 d}, \quad m = 0, 1, 2, 3 \dots (4)$$

$$\varepsilon_r = n/z_w, \quad \mu_r = n z_w, \quad (5)$$

where  $m$  is the branch index value. The correct sign for  $z_w$  in Eq. (3) can be chosen by applying  $\text{Re}\{z_w\} \geq 0$  indicating that the rate of heat dissipation in any passive medium [23]

$$Q = Q_{elec} + Q_{mag} > 0, \quad Q_{elec} = \omega \varepsilon_r'' \bar{E} \cdot \bar{E}^*, \quad Q_{mag} = \omega \mu_r'' \bar{H} \cdot \bar{H}^*, \quad (6)$$

must be positive where ‘\*’ denotes complex conjugate; and  $\text{Re}\{\cdot\}$  and  $\text{Im}\{\cdot\}$  are the real and imaginary operators, respectively. Besides, unique solution of  $n$  can be cast using different techniques in the literature through determination of correct  $m$  [10, 24–27].

### 3.2. Analytical Approach — Reference-plane Invariant

In previous subsection, it has been demonstrated that correct retrieval of  $\varepsilon_r$  and  $\mu_r$  is possible provided that reference-plane transformation factors  $R_1$  and  $R_2$  are precisely known. In what follows, we will illustrate that  $\varepsilon_r$  and  $\mu_r$  could be extracted using reference-plane invariant expressions. Toward this end, we let two new variables based on measured  $S$ -parameters and the slab length which is assumed to be known [14, 15]

$$A = \frac{S_{11}S_{22}}{S_{21}S_{12}} = \frac{\Gamma^2(1-T^2)^2}{T^2(1-\Gamma^2)^2}, \quad B = e^{2ik_0d} \frac{(S_{21}S_{12} - S_{11}S_{22})}{(S_{21}^0)^2} = \frac{T^2 - \Gamma^2}{1 - \Gamma^2 T^2}, \quad (7)$$

where  $S_{21}^0$  is the forward transmission  $S$ -parameter when there is no MM slab between calibration-planes. It is clear that the right sides of both expressions in Eq. (7) are independent of calibration-plane factors  $R_1$  and  $R_2$ . From Eq. (7), we obtain [14, 15]

$$\Gamma_{(1,2)}^2 = \frac{-\xi \mp \sqrt{\xi^2 - (2AB)^2}}{2AB}, \quad \xi = A(1+B^2) - (1-B)^2, \\ T = \frac{S_{21}R_0}{S_{21}^0} \frac{(1+\Gamma^2)}{1+B\Gamma^2}. \quad (8)$$

The correct sign of  $\Gamma^2$  in (8) can be selected by using the constraint  $|\Gamma| \leq 1$ , indicating the condition [23] given in Eq. (6). After determination of  $\Gamma^2$  and  $T$ , electromagnetic properties of isotropic MM slabs can be extracted from Eqs. (3)–(5). As pointed out before, unique solution of  $\varepsilon_r$  and  $\mu_r$  can be found using the techniques [10, 24–27].

Up to this point, we have assumed (as well as in the paper [14]) that correct solution of  $\Gamma$  from Eq. (8) using the constrain  $|\Gamma| \leq 1$  is possible. However, there are two roots of  $\Gamma$  which satisfy Eq. (8) since  $\Gamma = \pm\sqrt{\Gamma^2}$ . In this paper, we propose a simple tactic to resolve this issue as follows. First, we determine  $L_1$  or  $L_2$  from Eq. (1)

$$R_1^4 = S_{11}^2 \frac{(1 - \Gamma^2 T^2)^2}{\Gamma^2 (1 - T^2)^2}, \quad R_2^4 = S_{22}^2 \frac{(1 - \Gamma^2 T^2)^2}{\Gamma^2 (1 - T^2)^2}, \quad (9)$$

$$L_1 = \frac{\ln(R_1^4) \mp i2\pi p_1}{i4k_0}, \quad L_2 = \frac{\ln(R_2^4) \mp i2\pi p_2}{i4k_0}, \quad p_1, p_2 = 0, 1, 2, \dots \quad (10)$$

using determined unique expressions of  $\Gamma^2$  and  $T$  from Eq. (8). Determined  $L_1$  and  $L_2$  values from Eq. (10) will be real quantities since  $R_1$  and  $R_2$  in Eq. (2) are two exponential quantities having only an imaginary argument. Although it seems at first moment that there are also multiple solutions for  $L_1$  and  $L_2$ , using measurements at multiple frequencies and finding almost identical  $L_1$  and  $L_2$  values for all  $p_1$  and  $p_2$  in Eq. (10), this dilemma can be solved because  $L_1$  and  $L_2$  are physical properties not changing with frequency. Next, after determination of  $L_1$  and/or  $L_2$ , we obtain  $\Gamma$  from

$$\Gamma = \frac{S_{11}(1 - \Gamma^2 T^2)}{R_1^2(1 - T^2)} = \frac{S_{22}(1 - \Gamma^2 T^2)}{R_2^2(1 - T^2)}, \quad (11)$$

once  $\Gamma^2$ ,  $T$ , and  $R_1$  (or  $R_2$ ) values are substituted from Eqs. (8) and (10).

### 3.3. Dispersion Model Approach

This model is based upon using different dispersion models for extracting from synthesized  $S$ -parameters electromagnetic properties of isotropic MM slabs in Fig. 1. In this model, simulated or measured  $S$ -parameters are fitted to those obtained from Drude and Lorentz type dispersion models [19, 28] in which  $\varepsilon_r$  and  $\mu_r$  can be expressed

$$\varepsilon_r(\omega) = \varepsilon_\infty - \frac{\omega_{ep}^2}{\omega(\omega + i\delta_e)}, \quad \mu_r(\omega) = \mu_\infty - \frac{(\mu_s - \mu_\infty)\omega_{mp}^2}{\omega(\omega + i\delta_m) - \omega_{mp}^2}, \quad (12)$$

where  $\varepsilon_\infty$  is the electric permittivity at theoretically infinite frequency,  $\omega_{ep}$  the electronic plasma frequency,  $\delta_e$  the electronic damping coefficient,  $\mu_\infty(\mu_s)$  the magnetic permeability at theoretically infinite (zero) frequency,  $\omega_{mp}$  the magnetic plasma frequency, and  $\delta_m$  the magnetic damping coefficient. For isotropic MM slabs composed of only SRRs, we set  $\omega_{ep} = 0$  and  $\delta_e = 0$ .

This model works as follows [19]. First, ranges of possible solutions for  $\varepsilon_\infty$ ,  $\omega_{ep}$ ,  $\delta_e$ ,  $\mu_\infty$ ,  $\mu_s$ ,  $\omega_{mp}$ , and  $\delta_m$  are estimated. Next, for given or assumed values of  $\varepsilon_\infty$ ,  $\omega_{ep}$ ,  $\delta_e$ ,  $\mu_\infty$ ,  $\mu_s$ ,  $\omega_{mp}$ , and  $\delta_m$  within the range,  $\varepsilon_r$  and  $\mu_r$  are determined from Eq. (12). After, depending on using reference-plane dependent and reference-plane invariant  $S$ -parameter expressions, calculated  $\varepsilon_r$  and  $\mu_r$  are substituted into either Eq. (1) or (7) once upon  $\Gamma$  and  $T$  are determined from Eq. (2). Finally, a suitable optimization algorithm such as the differential evolution (DE) algorithm [19] or the “fmincon” function of MATLAB is selected to determine next seed of iteration until the simulated  $S$ -parameters are fitted within specified limits. Since the DE algorithm yields different solutions depending on values of initially arranged parameters, in our

paper we decided to apply the “fmincon” function provided that the range of values of  $\varepsilon_\infty$ ,  $\omega_{ep}$ ,  $\delta_e$ ,  $\mu_\infty$ ,  $\mu_s$ ,  $\omega_{mp}$ , and  $\delta_m$  are known. To be discussed later, their ranges can be estimated from extracted values using the analytical approach.

#### 4. SIMULATION RESULTS

We use the unit cell dimensions in [18] as for the dimensions of unit cells of our isotropic MM slabs with/without cut wires in Fig. 1 in our simulation analysis. While the cell with only SRRs is denoted by SRR isotropic MM slab as shorthand for the discussion of results in this paper, the cell with both SRRs and cut wire is designated by Composite isotropic MM slab for the same goal. The dimensions of each unit cell are  $a_x = 8.8$  mm,  $a_y = 6.5$  mm, and  $d = 8.8$  mm. The substrate made up by the FR-4 dielectric material ( $\varepsilon_r = 4.4$  and conductance of  $0.0068$  S/m) has a thickness of  $1.6$  mm. Geometric parameters of SRRs are  $g = t = 0.2$  mm,  $w = 0.9$  mm, and  $r = 1.6$  mm, while that of cut wire is  $w = 0.9$  mm. The patterns of copper, with an assumed electrical conductivity of  $5.8 \times 10^7$  S/m, are  $30 \mu\text{m}$  thick. Different lossy isotropic MM slabs with/without cut wires are achieved by varying the value of conductance of the substrate to analyze effects of lossy nature of isotropic MM slabs in the extraction of their electromagnetic properties. We utilize the CST Microwave Studio simulation program based on finite integration technique [29] to simulate  $S$ -parameters for each unit cell in Fig. 1. Whereas periodic boundary conditions are used along  $x$ - and  $y$ -directions, waveguide ports are assumed along  $z$ -direction. For more details about simulations, the reader can refer to [29]. For conciseness, simulated  $S$ -parameters over  $f = 2\text{--}5$  GHz of the SRR and Composite MM slabs with substrate conductance ( $\sigma$ ) of  $0.0068$  S/m and  $L_1 = 0 = L_2$  are given in Fig. 2.

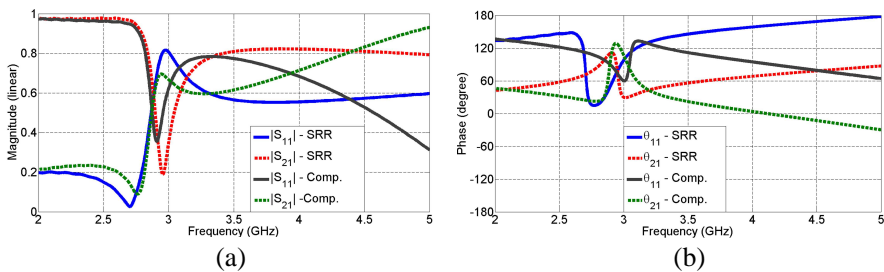


**Figure 2.** (a) Magnitude and (b) phase of the simulated  $S$ -parameters for the SRR and Composite MM slabs with substrate conductance of  $0.0068$  S/m and  $L_1 = 0 = L_2$  ( $S_{11} = S_{22}$ ).

## 5. RETRIEVED ELECTROMAGNETIC PROPERTIES

Here, we present retrieved electromagnetic properties of isotropic SRR and Composite MM slabs with different  $\sigma$  values from their simulated  $S$ -parameters, some of which are illustrated in Fig. 2. We apply three different approaches for retrieval process and consider reference-plane invariant expressions in some cases. The first and second approaches are based upon extraction of electromagnetic properties from explicit analytical expressions [9, 10, 14, 15], while the third approach uses dispersion models (Lorentz and Drude [19, 28]) to predict accurate electromagnetic properties [19]. Advantages and drawbacks of each approach will be discussed wherever appropriate.

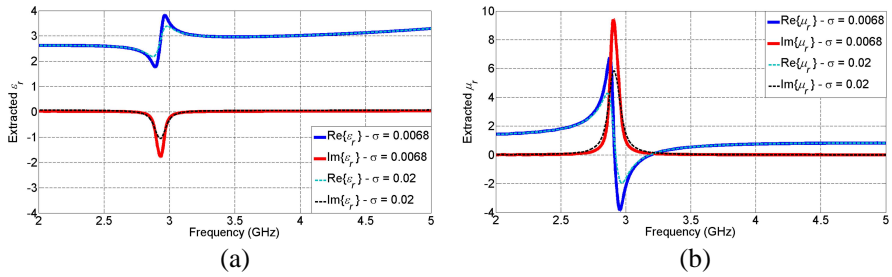


**Figure 3.** Extracted (a) permittivity and (b) permeability of the SRR MM slab with various substrate conductance values (S/m) and  $L_1 = 0 = L_2$  using the first approach.

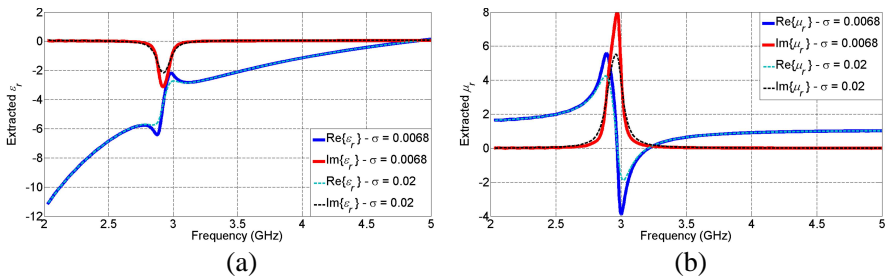


**Figure 4.** Extracted (a) permittivity and (b) permeability of the Composite MM slab with various substrate conductance values (S/m) and  $L_1 = 0 = L_2$  using the first approach.



### 5.1. First Analytical Approach — Reference-plane Dependent

Using derived expressions in Eqs. (3)–(5) and simulated  $S$ -parameters, we extracted  $\varepsilon_r$  and  $\mu_r$  of isotropic SRR and Composite MM slabs with various  $\sigma$ ,  $L_1$ , and  $L_2$  values. In Figs. 3 and 4, we demonstrate over 2–5 GHz the retrieved  $\varepsilon_r$  and  $\mu_r$  of SRR and Composite MM slabs with  $\sigma = 0.0068$  S/m to reproduce the simulation results in Figs. 6(c), 6(d), 8(c), and 8(d) of the paper [18]. The relative shifts near resonance regions in extracted  $\varepsilon_r$  and  $\mu_r$  dependences between our simulated results and those in [18] can arise from location of metallic structures within the cell. It is noted from Figs. 3 and 4 that while the extracted  $\varepsilon'_r$  demonstrates anti-resonant behavior near the resonance region ( $f \cong 2.9$  GHz), the extracted  $\mu'_r$  shows resonant behavior near the same region for both SRR and Composite MM slabs. Furthermore,

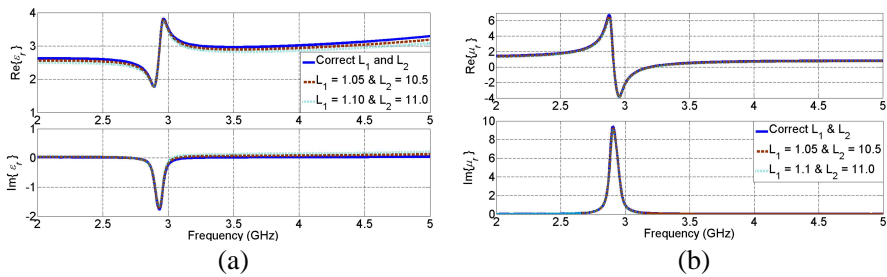


**Figure 5.** Extracted (a) permittivity and (b) permeability of the SRR MM slab with  $\sigma = 0.0068$  (S/m) and various lengths (mm) using the first approach [correct parameters are  $L_1 = 1$  mm and  $L_2 = 10$  mm].

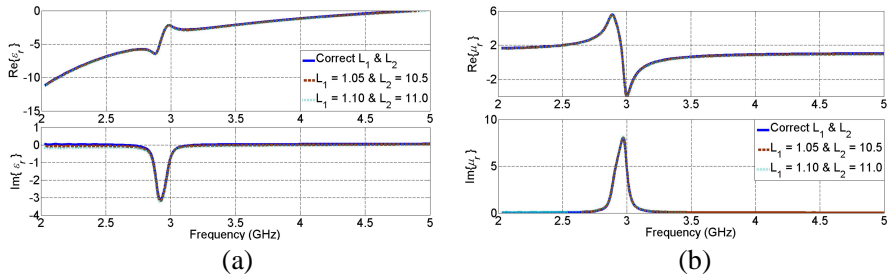


**Figure 6.** Extracted (a) permittivity and (b) permeability of the Composite MM slab with  $\sigma = 0.0068$  (S/m) and various lengths (mm) using the first approach [correct parameters are  $L_1 = 1$  mm and  $L_2 = 10$  mm].

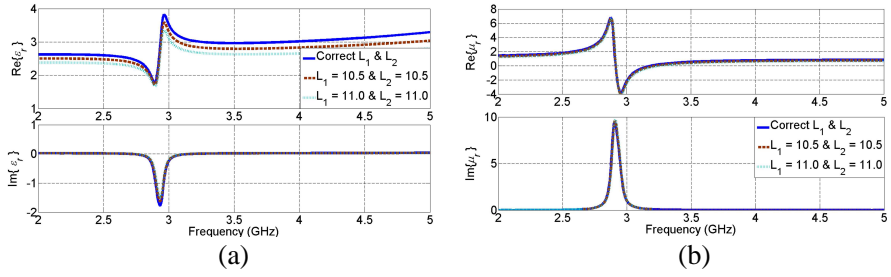


**Figure 7.** Extracted (a) permittivity and (b) permeability of the SRR MM slab with  $\sigma = 0.0068$  (S/m) and various lengths (mm) using the first approach [correct parameters are  $L_1 = 10$  mm and  $L_2 = 10$  mm].

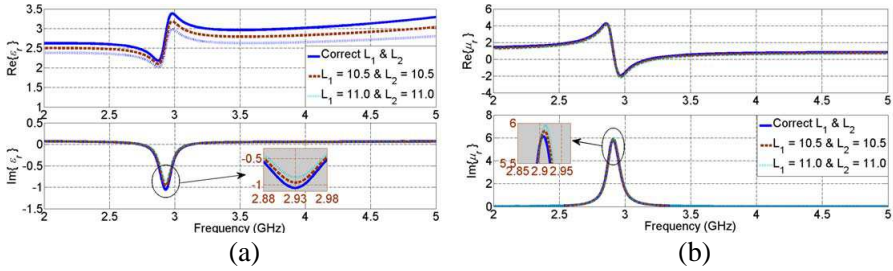


**Figure 8.** Extracted (a) permittivity and (b) permeability of the SRR MM slab with  $\sigma = 0.020$  (S/m) and various lengths (mm) using the first approach [correct parameters are  $L_1 = 10$  mm and  $L_2 = 10$  mm].

the extracted  $\epsilon$  and  $\mu$  appear in conjugate form, namely, the extracted  $\epsilon_r''$  is less than zero near the resonance region, whereas  $\mu_r''$  is greater than zero over the whole frequency region for both SRR and Composite MM slabs. However, the retrieved  $\epsilon_r''$  near the resonance region does not comply with the second principle of thermodynamics [23]. In Subsection 5.3, we will discuss how this unphysical artifact can be eliminated. Finally, it is seen from Figs. 3 and 4 that an increase in  $\sigma$  value, indicating that the cell becomes lossy, decreases not only the intensity of electric and magnetic responses near resonance region but also decreases the possibility of violation of the second principle of thermodynamics. This effect of  $\sigma$  is in complete agreement with quality factor of resonating structures, where loss present inside them decreases their resonance behavior, since MM slabs in Fig. 1 can be considered as resonating structures [29,30]. In the dependencies in Figs. 3 and 4, we assumed that the MM slab end faces overlap exactly with calibration-planes. However, in real measurements, such a requirement

is not easily and always met. Therefore, an experimentalist should consider consequences of any incorrect data of  $L_1$  and  $L_2$  (Fig. 1) on dependencies of the extracted  $\varepsilon_r$  and  $\mu_r$ . For example, Figs. 5–8 show some simulation results for monitoring effects of inaccurately measured  $L_1$  and/or  $L_2$  on the extracted  $\varepsilon_r$  and  $\mu_r$  of MM slabs with  $\sigma = 0.0068$  S/m and  $\sigma = 0.020$  S/m.

General conclusions we draw from simulations in this subsection are given as follows:

- a) When offsets from true values of  $L_1$  and  $L_2$  increase, the retrieved  $\varepsilon_r$  and  $\mu_r$  (barely perceived in the plots) diverge accordingly from their actual values with reference to correct  $L_1$  and  $L_2$  (Figs. 5 and 7). This divergence augments with an increase in  $L_1$  and  $L_2$  values (Figs. 5 and 7), arising from increased phase differences with offset in periodic manner on account for complex exponential  $R_1$  and  $R_2$  in Eq. (2).
- b) We see from Figs. 5–8 that  $\mu_r$  is almost insensitive to changes in  $L_1$  and  $L_2$ ; but  $\varepsilon_r$  noticeably decreases as  $L_1$  and  $L_2$  are increased. So the magnetic response does not depend on  $\varepsilon_r$ , and then we can infer that electric and magnetic responses are uncoupled for our study. The decrease of  $\varepsilon_r$  with increasing  $L_1$  and  $L_2$  can be explained by fact that adding two layers of air (of lengths  $L_1$  and  $L_2$ ) to the dielectric substrate increases the volume of the dielectric via an increase in effective slab length ( $d_{eff} > d$ ), and averaging over the increased volume yields a lower  $\varepsilon_r$ .
- c) While offsets from true values of  $L_1$  and  $L_2$  generally affect  $\text{Re}\{\varepsilon_r\}$  and  $\text{Re}\{\mu_r\}$  over whole frequency region, they just barely alter  $\text{Im}\{\varepsilon_r\}$  and  $\text{Im}\{\mu_r\}$  in the resonance region (see the insets in Fig. 8). This effect arises from the fact that  $\text{Re}\{\varepsilon_r\}$  and  $\text{Re}\{\mu_r\}$  are mainly influenced by a phase shift, whereas  $\text{Im}\{\varepsilon_r\}$  and  $\text{Im}\{\mu_r\}$  are chiefly altered by an amplitude change for low-loss materials [31].
- d) Effects of offsets from true of  $L_1$  and  $L_2$  are generally lower near resonance region for Composite MM slabs than for SRR MM slabs (Figs. 5 and 6) because inclusion of metallic lossy cut wire decreases quality of the resonating Composite MM slab, reducing the frequency rate of change of  $S$ -parameters and thus  $\varepsilon_r$  and  $\mu_r$  [29].
- e) We note from Figs. 3(a), 4(a), 5(a), 6(a), 7(a), and 8(a) that retrieved  $\text{Im}\{\varepsilon_r\}$  values are negative near resonance region ( $f \cong 2.9$  GHz) for both SRR and Composite MM slabs, violating the passivity condition in Eq. (6) [23]. This problem (violation of locality conditions) arises from spatial dispersion effects due to

discreteness of conducting elements repeated periodically in a non-homogeneous metamaterial bulk [16, 18, 19]. These effects mostly result in large values of permittivity and permeability, when the amplitude and phase of fields inside a medium vary quickly (e.g., resonance region).

- f) General results discussed in (a), (b) and (c) apply to Composite MM slabs whose electromagnetic property dependence is not shown for conciseness.

## 5.2. Second Analytical Approach — Reference-plane Invariant

In a manner similar to the case in the previous subsection, we utilize analytical expressions, but reference-plane invariant ones from Eqs. (7)–(11), to extract  $\varepsilon_r$  and  $\mu_r$  of isotropic SRR and Composite MM slabs with various  $\sigma$ ,  $L_1$ , and  $L_2$  values. From our simulations, we find the following results:

- a) Retrieved electromagnetic properties of isotropic SRR and Composite MM slabs with  $\sigma = 0.0068 \text{ S/m}$  and  $\sigma = 0.02 \text{ S/m}$  for various  $L_1$  and  $L_2$  are identical to those corresponding to correct  $L$  values in Figs. 3–8 (not repeated for brevity). This means that reference-plane invariant analytical expressions for extraction of electromagnetic properties eliminate any errors arising from inaccurate knowledge of  $L_1$  and  $L_2$ .
- b) In addition to eliminating of artificial changes in retrieved  $\varepsilon_r$  and  $\mu_r$  (general result (c) in Subsection 5.1), reference-plane invariant expressions remove unreal electric and magnetic resonant behavior (general result (b) in Subsection 5.1).
- c) Retrieved  $\text{Im}\{\varepsilon_r\}$  values of isotropic SRR and Composite slabs still have negative values near resonance region ( $f \cong 2.9 \text{ GHz}$ ). Its reason parallels with that given in general results (e) in Subsection 5.1, because reference-plane invariant analytical expressions also utilize simulated  $S$ -parameters without regarding the accuracy of simulated  $S$ -parameters near resonance region due to discreteness of periodic elements.

## 5.3. Retrieval by the Dispersion Model Approach

In the previous two subsections, we noted that extracted  $\text{Im}\{\varepsilon_r\}$  values of isotropic SRR and Composite MM slabs by both analytical approaches become negative near resonance region, and this is physically incorrect if the rate of heat dissipation of any passive medium is considered. To resolve this problem, in this subsection we

utilize dispersion model approach where Lorentz and Drude dispersion type models in Eq. (12) are utilized for SRR and Composite MM slabs. Incorporating these models with simulated  $S$ -parameters in Fig. 2, as shown in Figs. 9 and 10, we retrieved the  $\varepsilon_r$  and  $\mu_r$  over 2–5 GHz of isotropic SRR and Composite MM slabs with various  $\sigma$ ,  $L_1$ , and  $L_2$  values using reference-plane invariant expressions in Eqs. (7)–(11), since the effect of inaccurate knowledge of  $L_1$  and  $L_2$  is investigated in Subsection 5.1, and since in this subsection our main concern is to eliminate inaccuracies occurring from  $\text{Im}\{\varepsilon_r\} < 0$  in Figs. 3(a)–8(a). The dispersion model approach not only extracts physically correct  $\varepsilon_r$  and  $\mu_r$ , but also determines the electromagnetic parameters as tabulated in Table 1. In electromagnetic parameters determination in Table 1, we applied the “fmincon” function and utilized dependencies in Figs. 3 and 4 to assign ranges for the parameters

$$1 \leq \varepsilon_\infty \leq 5, \quad 0 \leq \delta_e, \delta_m \leq 5, \quad 1 \leq \mu_s, \mu_\infty \leq 2. \quad (13)$$

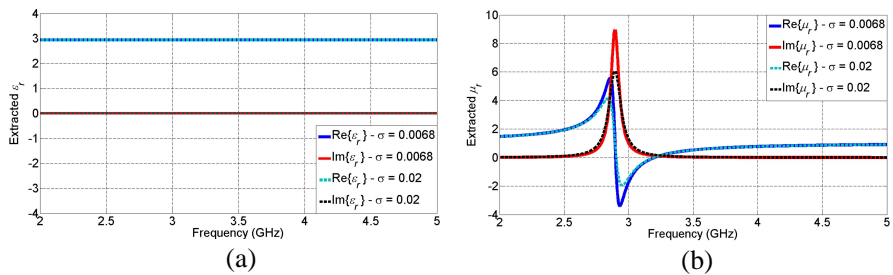


**Figure 9.** Extracted (a) permittivity and (b) permeability of the SRR MM slab with various substrate conductance values (S/m) and different values of  $L_1$  and  $L_2$  using dispersive model approach.

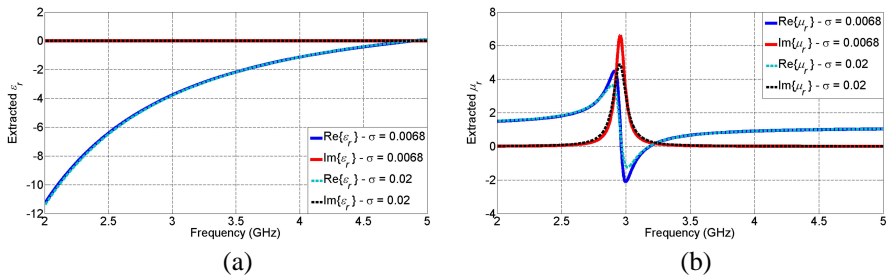


**Figure 10.** Extracted (a) permittivity and (b) permeability of the Composite MM slab with various substrate conductance values (S/m) and different values of  $L_1$  and  $L_2$  using dispersive model approach.

**Table 1.** Electromagnetic parameters of MM slabs in Fig. 1 obtained from the dispersion model.

MM slab	$\varepsilon_\infty$	$\omega_{ep}$ (GHz)	$\delta_e$ (GHz)	$\mu_s$	$\mu_\infty$	$\omega_{mp}$ (GHz)	$\delta_m$ (GHz)
SRR ( $\sigma = 0.0068$ )	2.938	-	-	1.265	1.032	18.181	0.472
SRR ( $\sigma = 0.02$ )	2.939	-	-	1.261	1.027	18.182	0.698
Comp. ( $\sigma = 0.0068$ )	2.258	46.271	0.206	1.334	1.141	18.577	0.542
Comp. ( $\sigma = 0.02$ )	2.313	46.622	0.260	1.347	1.147	18.557	0.757

Comparing Figs. 3 and 4 with Figs. 9 and 10, we see that the dispersion model approach removes superfluous resonant behavior of  $\varepsilon_r$  for both SRR and Composite MM slabs around  $f \cong 2.9$  GHz and in turn makes the retrieved  $\varepsilon_r$  physically meaningful. Furthermore, it also slightly decrease the resonant behavior of  $\mu_r$  in favor of making  $\text{Im}\{\varepsilon_r\} \geq 0$ . Finally, it is noted from Table 1 that an increase in  $\sigma$  augments both  $\delta_e$  and  $\delta_m$  for both SRR and Composite MM slabs.

## 6. CONCLUSIONS

We have applied three methods for constitutive parameters measurement of SRR and Composite MM slabs when slab surfaces do not match with calibration planes. First, two different methods depending on whether they require the knowledge of calibration-plane factors, based on closed-form analytical expressions are utilized. Second, a method relied on Lorentz and Drude models is adopted for reference-plane invariant constitutive parameters determination. We have compared each method with one another using simulated  $S$ -parameters of two typical SRR and Composite MM slabs with various losses and different calibration plane factors. From the comparison, we note that whereas both of the applied analytical methods produce unphysical  $\varepsilon_r$  (but physical  $\mu_r$ ) near resonance regions, the approach based on Lorentz and Drude models eliminates this problem and extracts correct constitutive parameters over whole band. It is noted that retrieved unphysical  $\varepsilon_r$  is due to spatial dispersion effects arising from discreteness of conducting parts of MM slabs, thereby altering simulated  $S$ -parameters considerably.

## REFERENCES

1. Pendry, J. B., A. J. Holden, D. J. Robbins, and W. J. Stewart, "Low frequency plasmons in thin-wire structures," *J. Phys.: Condens. Matter*, Vol. 10, 4785–4809, 1998.
2. Lindell, I. V., S. A. Tretyakov, K. I. Nikoskinen, and S. Ilvonen, "BW media-media with negative parameters, capable of supporting backward waves," *Microw. Opt. Technol. Lett.*, Vol. 31, 129–133, 2001.
3. Engheta, N., "An idea for thin subwavelength cavity resonators using metamaterials with negative permittivity and permeability," *IEEE Antennas Wireless Propagat. Lett.*, Vol. 1, 10–13, 2002.
4. Alu, A. and N. Engheta, "Radiation from a travelling-wave current sheet at the interface between a conventional material and a metamaterial with negative permittivity and permeability," *Microw. Opt. Technol. Lett.*, Vol. 35, No. 6, 460–463, 2002.
5. Duan, Z., B.-I. Wu, S. Xi, H. Chen, and M. Chen, "Research progress in reversed Cherenkov radiation in double-negative metamaterials," *Progress In Electromagnetics Research*, Vol. 90, 75–87, 2009.
6. Oraizi, H., A. Abdolali, and N. Vaseghi, "Application of double zero metamaterials as radar absorbing materials for the reduction of radar cross section," *Progress In Electromagnetics Research*, Vol. 101, 323–337, 2010.
7. Cojocaru, E., "Electromagnetic tunneling in lossless trilayer stacks containing single-negative metamaterials," *Progress In Electromagnetics Research*, Vol. 113, 227–249, 2011.
8. Alu, A., "First-principles homogenization theory for periodic metamaterials," *Phys. Rev. B*, Vol. 84, 075153, 2011.
9. Nicolson, A. M. and G. Ross, "Measurement of the intrinsic properties of materials by time-domain techniques," *IEEE Trans. Instrum. Meas.*, Vol. 19, No. 4, 377–382, 1970.
10. Weir, W. B., "Automatic measurement of complex dielectric constant and permeability at microwave frequencies," *Proc. IEEE*, Vol. 62, No. 1, 33–36, 1974.
11. Boughriet, A.-H., C. Legrand, and A. Chapoton, "Noniterative stable transmission/reflection method for low-loss material complex permittivity determination," *IEEE Trans. Microw. Theory Tech.*, Vol. 45, No. 1, 52–57, 1997.
12. Hasar, U. C. and C. R. Westgate, "A broadband and stable method for unique complex permittivity determination of low-loss materials," *IEEE Trans. Microw. Theory Tech.*, Vol. 57, No. 2,

- 471–477, 2009.
13. Barroso, J. J. and A. L. de Paula, “Retrieval of permittivity and permeability of homogeneous materials from scattering parameters,” *Journal of Electromagnetic Waves and Applications*, Vol. 24, Nos. 11–12, 1563–1574, 2010.
  14. Chalapat, K., K. Sarvala, J. Li, and G. S. Paraoanu, “Wideband reference-plane invariant method for measuring electromagnetic parameters of materials,” *IEEE Trans. Microw. Theory Tech.*, Vol. 57, No. 9, 2257–2267, 2009.
  15. Hasar, U. C. and Y. Kaya, “Reference-independent microwave method for constitutive parameters determination of liquid materials from measured scattering parameters,” *Journal of Electromagnetic Waves and Applications*, Vol. 25, Nos. 11–12, 1708–1717, 2011.
  16. Smith, D. R., S. Schultz, P. Markos, and C. M. Soukoulis, “Determination of effective permittivity and permeability of metamaterials from reflection and transmission coefficients,” *Phys. Rev. B*, Vol. 65, 195104, 2002.
  17. Chen, X., T. M. Grzegorzczuk, B.-I. Wu, J. Pacheco, Jr., and J. A. Kong, “Robust method to retrieve the constitutive effective parameters of metamaterials,” *Phys. Rev. E*, Vol. 70, 016608, 2004.
  18. Li, Z., K. Aydin, and E. Ozbay, “Determination of the effective constitutive parameters of bianisotropic metamaterials from reflection and transmission coefficients,” *Phys. Rev. E*, Vol. 79, 026610, 2009.
  19. Lubkowski, G., R. Schuhmann, and T. Weiland, “Extraction of effective metamaterial parameters by parameter fitting of dispersive models,” *Microw. Opt. Technol. Lett.*, Vol. 49, No. 2, 285–288, 2007.
  20. Markos, P. and C. M. Soukoulis, “Transmission properties and effective electromagnetic parameters of double negative metamaterials,” *Opt. Express*, Vol. 11, 649–661, 2003.
  21. Hasar, U. C. and J. J. Barroso, “Retrieval approach for determination of forward and backward wave impedances of bianisotropic metamaterials,” *Progress In Electromagnetics Research*, Vol. 112, 109–124, 2011.
  22. Shelby, R. A., D. R. Smith, S. C. Nemat-Nasser, and S. Schultz, “Microwave transmission through a two-dimensional, isotropic, left-handed metamaterial,” *Appl. Phys. Lett.*, Vol. 78, No. 4, 489–491, 2001.



23. Mattiucci, N., G. D'Aguanno, N. Akozbek, M. Scalora, and M. J. Blomer, "Homogenization procedure for a metamaterial and local violation of the second principle of thermodynamics," *Opt. Commun.*, Vol. 283, 1613–1620, 2010.
24. Szabo, Z., G.-H. Park, R. Hedge, and E.-P. Li, "Unique extraction of metamaterial parameters based on Kramers-Kronig relationship," *IEEE Trans. Microw. Theory Tech.*, Vol. 58, 2646–2653, 2010.
25. Barroso, J. J. and U. C. Hasar, "Resolving phase ambiguity in the inverse problem of transmission/reflection measurement methods," *Int. J. Infrared Milli. Waves*, Vol. 32, 857–866, 2011.
26. Luukkonen, O., S. I. Maslovski, and S. A. Tretyakov, "A stepwise Nicolson-Ross-Weir-based material parameter extraction method," *IEEE Antennas Propag. Lett.*, Vol. 10, 1295–1298, 2011.
27. Hasar, U. C., J. J. Barroso, C. Sabah, and Y. Kaya, "Resolving phase ambiguity in the inverse problem of reflection-only measurement methods," *Progress In Electromagnetics Research*, Vol. 129, 405–420, 2012.
28. Sabah, C. and S. Uckun, "Multilayer system of Lorentz/Drude type metamaterials with dielectric slabs and its application to electromagnetic filters," *Progress In Electromagnetics Research*, Vol. 91, 349–364, 2009.
29. Hasar, U. C., J. J. Barroso, M. Ertugrul, C. Sabah, and B. Cavusoglu, "Application of a useful uncertainty analysis as a metric tool for assessing the performance of electromagnetic properties retrieval methods of bianisotropic metamaterials," *Progress In Electromagnetics Research*, Vol. 128, 365–380, 2012.
30. Xu, S., L. Yang, L. Huang, and H. Chen, "Experimental measurement method to determine the permittivity of extra thin materials using resonant metamaterials," *Progress In Electromagnetics Research*, Vol. 120, 327–337, 2011.
31. Hasar, U. C., "A new method for evaluation of thickness and monitoring its variation of medium- and low-loss materials," *Progress In Electromagnetics Research*, Vol. 94, 403–418, 2009.